



Triboelectric nanogenerators stimulated electroacupuncture (EA) treatment for promoting the functional recovery after spinal cord injury

Xuelian Wei ^{1,2,#}, Yunhang Wang ^{3,#}, Botao Tan ^{3,#}, Enyang Zhang ^{1,2},
 Baocheng Wang ^{1,2}, Hong Su ³, Lehua Yu ³, Ying Yin ^{3,*}, Zhong Lin Wang ^{1,2,4,*},
 Zhiyi Wu ^{1,2,*}

¹ Beijing Institute of Nanoenergy and Nanosystems, Chinese Academy of Sciences, Beijing 101400, China

² School of Nanoscience and Technology, University of Chinese Academy of Sciences, Beijing 100049, China

³ Department of Rehabilitation Medicine, The Second Affiliated Hospital of Chongqing Medical University, Chongqing 400010, China

⁴ School of Materials Science and Engineering, Georgia Institute of Technology, Atlanta, GA 30332, USA

Electroacupuncture (EA), as a particular type of electrostimulation treatment, has an extensive application in the field of biomedicine. Triboelectric nanogenerator (TENG) has sparked significant concern attributed to the high electrical output with low cost, whose electrical signals can also be directly usable for electrical stimulation. Here we propose a Chinese medicine EA treatment with the assistance of TENG technology, in which a bidirectional continuous current from a soft-contact freestanding rotary TENG (FR-TENG) is applied to two effective acupoints of rats by inserting electric needles. The TENG-driven EA treatment promotes the performance of gait 2 weeks after as well as the Basso–Beattie–Bresnahan (BBB) score. This elevation last as long as 4 weeks post injury. Moreover, the TENG-driven EA treatment enhances neuron survival in the ventral horn and inhibits astrocyte activation in the lesion site. Therefore, the TENG-driven EA treatment provides a significant neuroprotection effect on spinal cord contusion in rats. Our studies not only demonstrate the possibility of the TENG-driven EA treatment for traumatic central nervous system injuries but also provide an experimental basis for the prevention and treatment of diseases by traditional Chinese medicine treatment.

Keywords: Spinal cord injury; Electroacupuncture; Acupoints; Triboelectric nanogenerator; Direct electrostimulation

Introduction

Acupuncture is an important part of Chinese traditional medicine and is one of the widely recognized methods of treating diseases worldwide [1–4]. Numerous pieces of evidence show that acupuncture holds a significant therapeutic effect on neurological diseases, such as stroke, spinal cord injury (SCI), peripheral

nerve injury, and neurodegeneration [5–9]. A central idea of acupuncture in the treatment of human diseases is that stimulation at specific areas of the body (acupoints) can regulate human physiological functions through the conduction of meridians [10,11]. With obvious merits of stable efficacy, relatively simple operation, safety, and low cost, acupuncture treatment is widely accepted and trusted by the medical community. At present, doctors often need to combine acupuncture treatment with electrical stimulation to strengthen needle sensation (or Acesthesia) [4,12–15]. The combination of different current frequencies and discharge modes can be more targeted to the patient [16].

* Corresponding authors.

E-mail addresses: Yin, Y. (300735@cqmu.edu.cn), Wang, Z.L. (zhong.wang@mse.gatech.edu), Wu, Z. (wuzhiyi@binn.cas.cn).

Xuelian Wei, Yunhang Wang, Botao Tan contribute equally to this work.

Considering the relatively high cost and potential electrical risk of commercial electroacupuncture (EA) treatment devices, the triboelectric nanogenerator (TENG) is emerging with low cost, widely available materials, flexible structures, and miniaturization in the field of healthcare, and provides a new way for electric energy of medical electronics [17–20]. Meanwhile, a number of TENG-based devices are proliferating, aiming at the biomedical applications [21–26]. For TENGs, energy conversion is achieved through coupling effect between triboelectrification and electrostatic induction effects, with current flowing back and forth between the two electrodes [27–29]. Some pioneering work has demonstrated that electrical currents generated by TENG can directly stimulate biological tissues. Lee et al. introduced a novel water/air-hybrid TENG for peripheral nerve stimulation [30]. Besides, Hu et al. displayed a TENG-driven electric stimulation system, demonstrating that TENG stimulation regulates cell proliferation and migration at the level of gene expression [31]. Furthermore, Yao et al. designed a universal motion-activated and wearable electric stimulation device that can effectively promote hair regeneration [32]. For electrical muscle stimulation, Wang et al. developed a self-powered direct muscle stimulation system with a TENG as a power source and waveform generator, and confirmed that the electrical muscle stimulation efficiency is affected by the electrode-motoneuron position and the stimulation waveform polarity [33]. However, there is still a paucity of research on the direct stimulation of current generated by TENG to acupoints for treating central nervous system (CNS) injuries, such as SCI. In addition, compared with unidirectional current, the bidirectional current has fewer adverse effects [34,35].

Here, we present a Chinese medicine treatment with the assistance of TENG technology, which uses the bidirectional continuous current from TENGs to act on two key acupoints, Dazhui (GV14) and Mingmen (GV4), by inserting the milli-needles of rats. As a result, the method effectively promotes the recovery of the nervous system and function after SCI, relieves chronic pain and other complications, meanwhile, inhibits inflammation. Experiments further show that the TENG-driven EA system has a beneficial therapeutic effect on SCI. The TENG-driven EA treatment promotes the survival of ventral horn neurons and inhibits the activation of astrocytes at the lesion site, while overactivation is detrimental to spinal cord repair. Therefore, the TENG-driven EA treatment provides a significant neuroprotection against spinal contusion injury in rats. Furthermore, our behavior results demonstrate locomotion functional recovery in TENG-driven EA group. The TENG-based EA physiotherapy owns the potential clinical application prospects in the repair, treatment, and rehabilitation of spinal cord injury patients.

Results and discussion

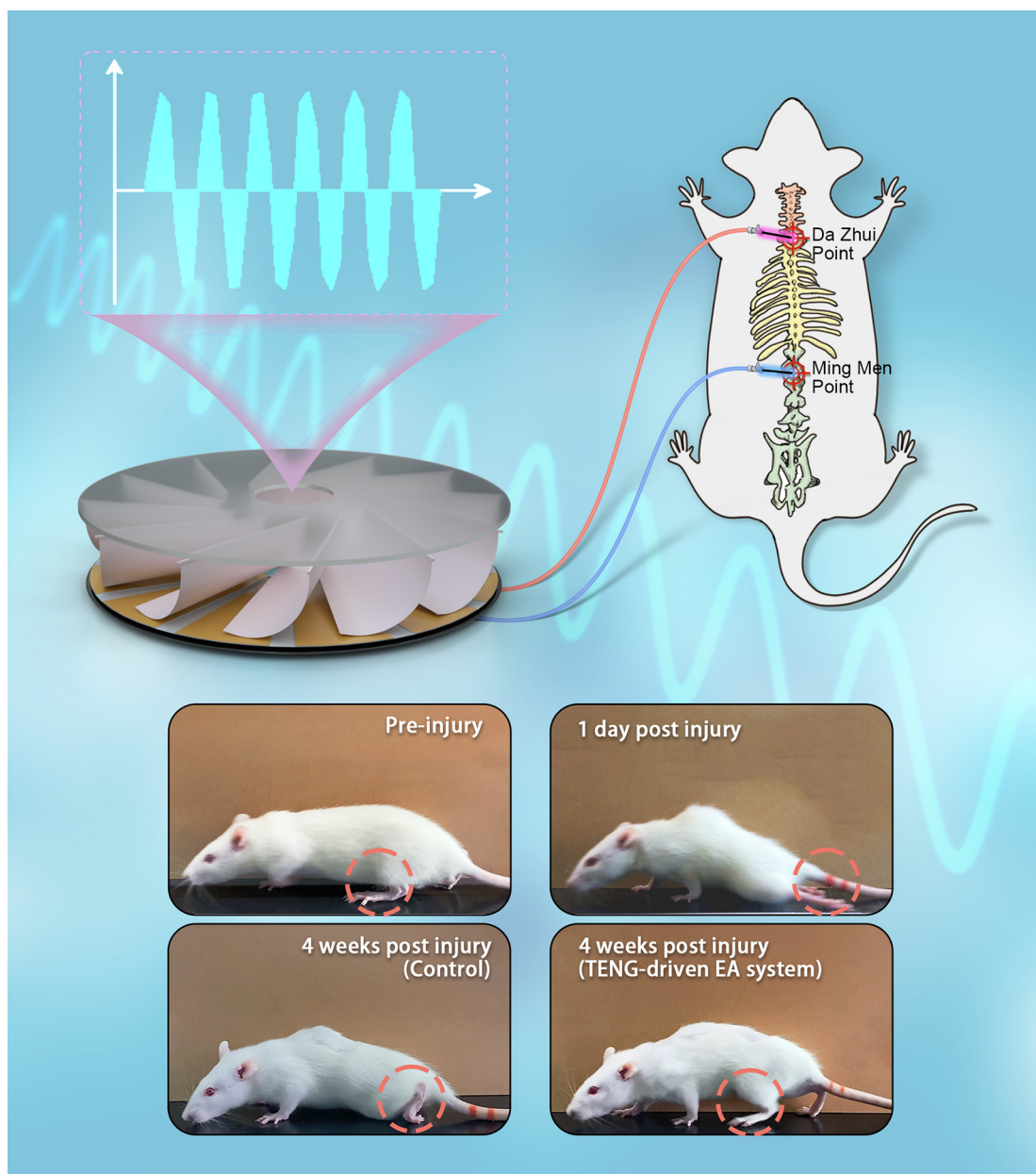
The concept of the TENG-driven EA treatment

SCI usually leads to irreversible tissue loss and neurological dysfunction, resulting in patients with long-term disabilities. The incidence of SCI is increasing and affects millions of individuals worldwide [36,37]. Electroacupuncture, which applies an electrical current to acupuncture needles after they have been inserted into the body, has a long history of clinical application for SCI in

China and worldwide [38,39]. Previous clinical studies have reported that EA treatment can contribute to neurologic and functional recoveries, and alleviate complications such as chronic pain and urinary incontinence for SCI patients [40–42]. Also, basic experimental studies confirmed that EA inhibits inflammation and promotes axonal regeneration and neural plasticity [43–47]. Among all those acupoints that work well in SCI patients, Dazhui (GV14) and Mingmen (GV4) are considered to be the most common and effective ones, especially in rodent studies [48,49]. Fig. 1 depicts direct EA treatment of two acupoints (Dazhui and Mingmen points) in the rat using a soft-contact freestanding rotary triboelectric nanogenerator (FR-TENG) as the current source. By comparing the optical images of pre-injury, 1 day post injury, 4 weeks post injury without any treatment, and 4 weeks post injury after TENG-driven EA treatment, it's visually evident that the hindlimbs of treated rats can stand again. This indicates that the TENG-driven EA treatment has a significant effect on the recovery of hindlimb locomotor function. A soft-contact FR-TENG with high current, wear-resistance, and the unique self-generation possibility is specifically designed as the power supply. The output current of the FR-TENG is applied directly to the relevant acupoints through acupuncture needles with a connecting transformer, so as to achieve the purpose of rehabilitation or treatment. The detailed preparation process of FR-TENG can be found in the Experimental Section. The soft-contact rotary structure is constructed to meet enough current range required for acupuncture and the treatment time of EA. In pre-experimental, we kept trying to find the appropriate conditions of current stimulation, so that the rats did not bray but the needle handles vibrated slightly. In this work, for the commercial EA instrument, a continuous wave of 100 Hz is used for EA treatment. And for the TENG-driven EA system, the output current can be adjusted by changing the rotation speed of the FR-TENG. To ensure the same frequency, the rotation speed of the FR-TENG is controlled at 500 rpm in the wave analysis (*Supplementary Note 1*). However, during the actual EA treatment, the needle handles of the TENG-driven EA system show obvious shaking when the rotation speed is 200–250 rpm. Therefore, the rotation speed of the FR-TENG is always controlled within this range for the subsequent experiments.

Fabrication, mechanism and performance of the soft-contact FR-TENG

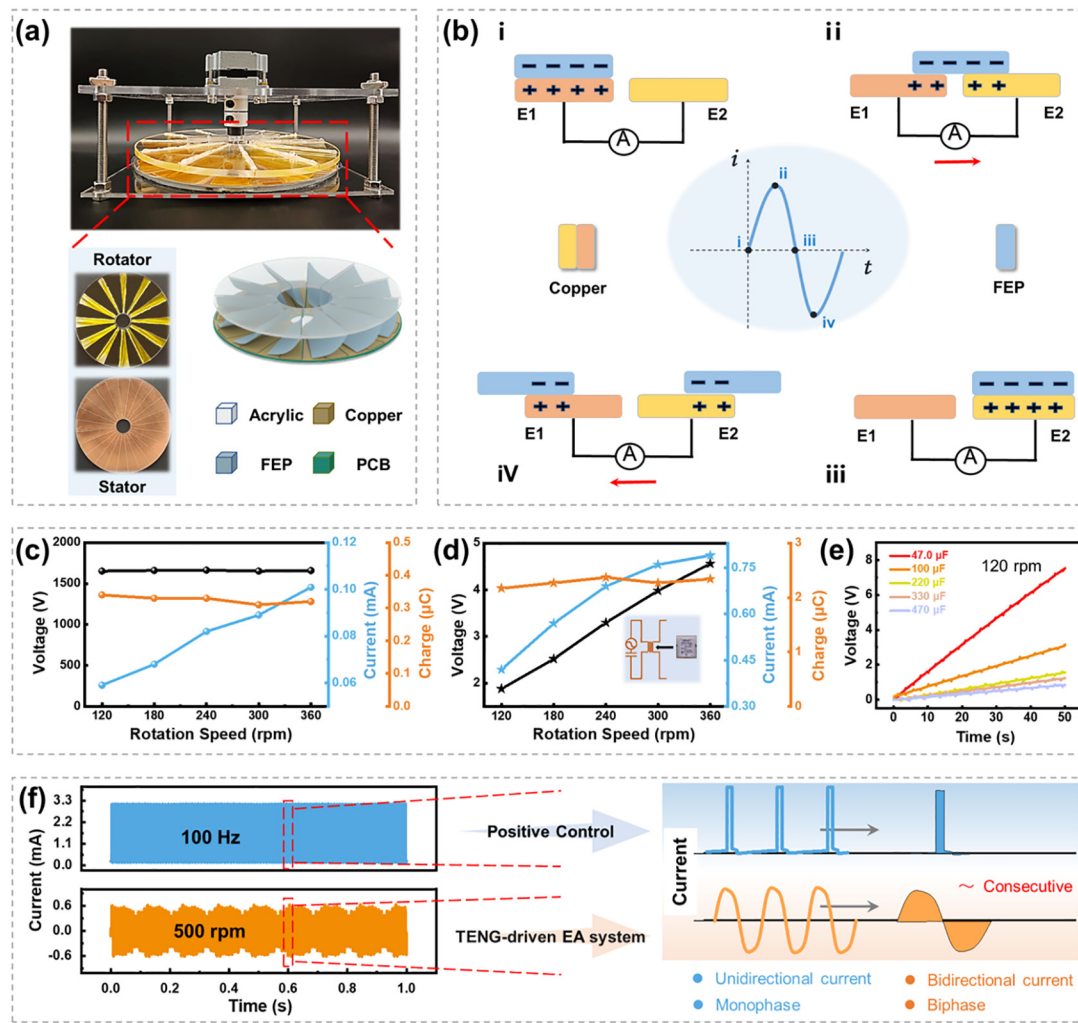
As a special form of electrical stimulation technique, EA has been applied in the field of biomedicine with good results. In view of the current stimulation with a certain amplitude of continuous wave/discontinuity wave required in the treatment process, and combined with the concept of self-powered biomedical equipment, a new type of continuous current source has attracted great attention. TENG has a broad application prospect as a new stimulation source. What's more, the electrical output of TENG has been proven to be directly used for electrical stimulation. However, there are few reports on the effectiveness of TENG-based current stimulation as a kind of EA physiotherapy in Chinese medicine. A soft-contact FR-TENG that can provide a large output current and the effect of long-term use is fabricated to generate a stimulated current. The PCB board with interdigital

**FIGURE 1**

Concept diagram of EA directly powered by a TENG for functional recovery after SCI. The TENG-driven EA system consists of a freestanding rotary triboelectric nanogenerator (FR-TENG) with a soft film structure, which provides stimulated current to act on two key acupoints in rats, namely, Dazhui (GV14) and Mingmen (GV4) points, respectively. Optical images of rats at different treatment times demonstrate the effectiveness of the system for functional recovery after SCI.

copper electrodes serves as the stator and the triboelectric layer, and twelve fluorinated ethylene propylene (FEP) blade-like films are connected with an acrylic sheet as the rotator and another triboelectric layer (Fig. 2a). A whole working process is shown in Fig. 2b, and an alternating current can be generated in the external circuit. At the initial state, the FEP film is completely covered on the Electrode 1 (E1), where negative charges are produced on the surface of the FEP film and equivalent quantity of positive charges are generated on the surface of the E1 (state i), due to the effect of triboelectrification. When the soft FEP film slides toward the Electrode 2 (E2), the generated positive charges on the surface of the E1 will gradually flow to the E2 through the

external circuit (state ii). As the first FEP film is fully slid on the surface of the E2, all the positive charges of the E1 will turn into the E2 (state iii). With the continuous rotation of the rotator, the first FEP film will slide across the E2, and the second FEP film will appear on this E1. At this point, a reverse current will be generated in the external circuit (state iv). The electrical output performance of the FR-TENG at different rotation speeds is measured, as shown in Fig. 2c. The results show that the I_{sc} increases continuously with the speed, while the V_{oc} and Q_{tr} remain a constant regardless of the rotation speed. To obtain a higher current amplitude to fulfill the EA treatment, a small transformer is used in the circuit (the circuit diagram shown in Fig. S2a). As shown in

**FIGURE 2**

Design, working principle, performance, and waveform analysis of the soft-contact FR-TENG. (a) Photograph and detailed structural information of the FR-TENG. (b) General working principle of the FR-TENG. Electrical output performance of the FR-TENG, including open circuit voltage (V_{oc}), short-circuit current (I_{sc}), and transferred charges (Q_{tr}) under various rotation speeds (c) before transformation and (d) after transformation. (e) Charging curves of different commercial capacitors at 120 rpm. (f) Waveforms of the commercial EA device (positive control) and the TENG-driven EA system.

Fig. 2d, the I_{sc} significantly increases after transformation. And at 240 rpm, the I_{sc} can reach 0.69 mA, which can fully reach the current range of the needle handles vibration. To ensure that the FR-TENG is not damaged by external factors (such as dust or rats) during the EA treatment, we fabricated a homemade acrylic container (Fig. S1a). The I_{sc} before and after transformation is also displayed in Fig. S1b (500 rpm). As a comparison, we use a commercial EA device as a positive control group (Fig. S1c), and the continuous wave mode at 100 Hz is applied in this experiment (Fig. S1d). The discontinuous wave and dilatational wave are also two common waveform modes, which still have remarkable therapeutic effects on some lesions, such as paraparesis, muscle weakness, and sciatica. That is going to be further investigated for future research. In addition, to further measure the output performance for practical applications, the charging curves of different capacitors charged by the FR-TENG at 120 rpm, 240 rpm, and 360 rpm are presented in Fig. 2e,

Fig. S2b, and Fig. S2c, respectively. Different capacitors can be charged quickly, which further indicates that the FR-TENG has the capacity to be a power source in terms of current output performance.

Commercial EA instruments are often put into use on the direct electrostimulation [50], the relevant electrical parameters (stimulation time, waveform, frequency, intensity) can be fine-tuned through knobs, thereby screening out the most appropriate acupuncture conditions. As shown in Fig. 2f, we briefly analyze the waveforms of a commercial EA device and a homemade TENG-driven EA system. After screening and experiments, we chose a continuous wave with a frequency of 100 Hz as the stimulated current of the commercial EA instrument, and the rotation speed of the TENG-driven EA device should be maintained at 500 rpm to ensure the same frequency with the former. The enlarged waveforms show that the output currents of both are continuous waves, despite the amplitude of the currents is differ-

ent. The difference is that the output of the commercial EA device is a unidirectional current, while the output of the TENG-driven EA system is a bidirectional current for biphasic electrostimulation. Considering the advantages of biphasic electrostimulation can maintain charge balance and reduce adverse reactions [34,35], the TENG-driven EA system is expected to be applied in clinical EA treatment after SCI.

The animal experimental design and TENG-driven EA treatment improved Basso–Beattie–Bresnahan (BBB) score

To investigate whether the TENG-driven EA treatment has therapeutic benefits for SCI, rats were subjected to a T10 contusion injury (Fig. S3a) followed by EA treatment for two weeks. The timeline is shown in Fig. 3a. Immediate after contusion, ischemia and edema originated around the wound in the spinal cord

(Fig. 3b and c). All SCI rats showed hindlimb paralysis (BBB scored 0) (Fig. 3d and g). Epicenter present in Fig. 3e. The rats in the positive control and TENG-driven EA group were bound in a prone position and received EA treatment at Dazhui (GV14) and Mingmen (GV4) without anesthesia, respectively (Fig. 3f). We observed short and mild, hindlimb flexion when EA was applied. The 21 scoring BBB system is used to assess the recovery of hindlimb locomotor function in SCI rats. Except the sham group, the BBB score of all rats was significantly dropped to zero (no observable hindlimb movement) on day 1 (Fig. S3b) and slowly rebounded within the following weeks after SCI (Fig. 3g). However, the BBB score in the TENG-driven EA group and the positive control group increased significantly compared to the control group from the first week. The statistic differences were found at 3 wpi and 4 wpi (Control group vs

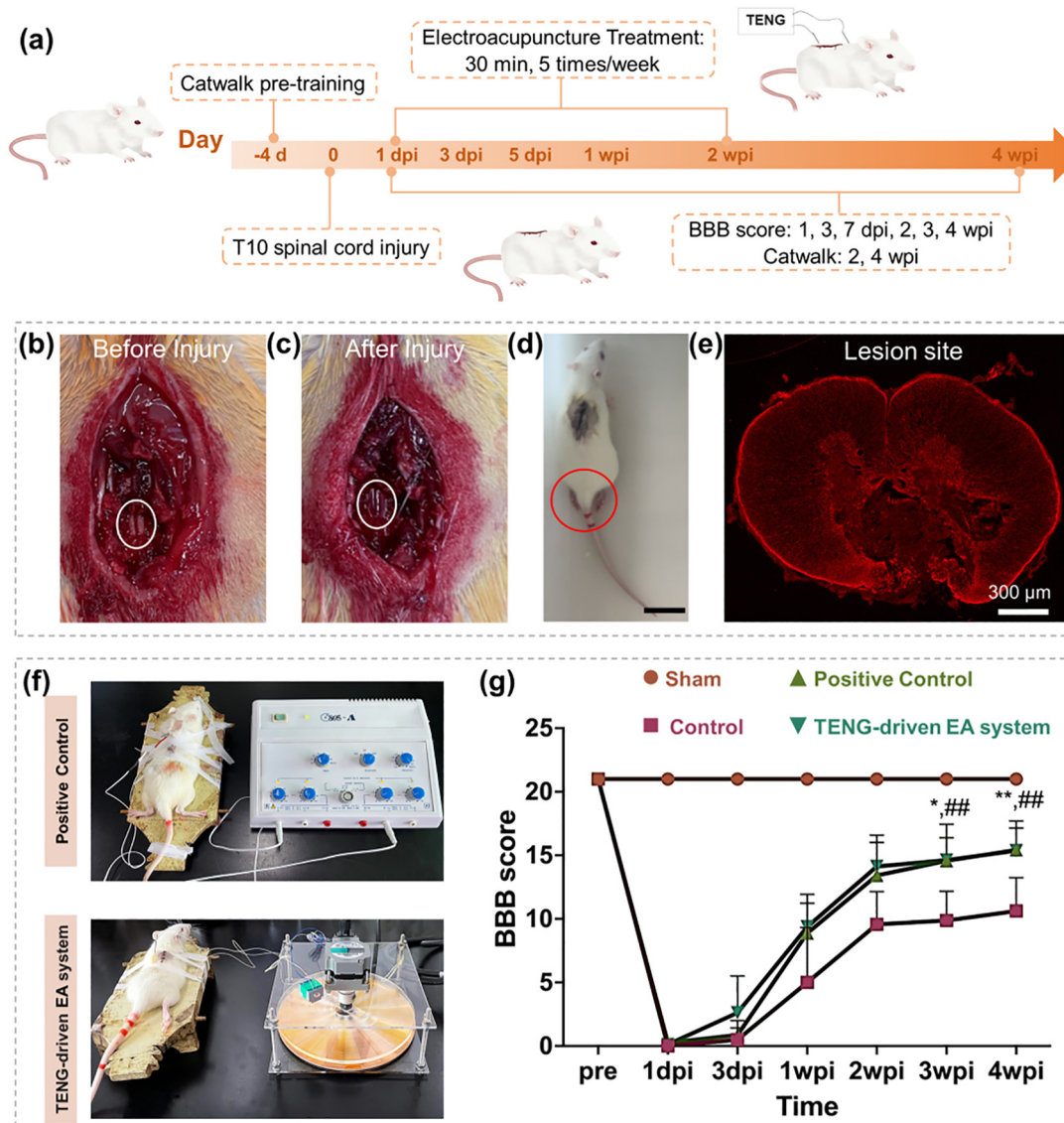


FIGURE 3

The experimental design and the hindlimb locomotor recovery. (a) The illustration of experimental timeline (1 dpi: 1 day post injury; 1 wpi: 1 week post injury); Representative images of (b) intact and (c) injured spinal cord; (d) SCI rat; (e) Representative fluorescence images of transverse spinal cord sections in the epicenter showing GFAP (red). Bar = 300 μm; (f) EA treatment of the positive control and TENG-driven EA system group; (g) BBB score of all groups after SCI. Data presented as mean ± SD ($n = 8$ per group). * $p < 0.05$, ** $p < 0.01$ for TENG-driven EA group versus control group; # $p < 0.05$, ## $p < 0.01$ for positive control group versus control group as determined by two-way ANOVA followed post hoc Tukey's test.

TENG-driven EA group: 3 wpi, 9.875 ± 2.295 vs 14.625 ± 2.825 , $p = 0.0121$; 4 wpi, 10.625 ± 2.615 vs 15.375 ± 2.326 , $p = 0.0088$; control group vs positive control group: 3 wpi, 9.875 ± 2.295 vs 14.571 ± 1.812 , $p = 0.0034$; 4 wpi, 10.625 ± 2.615 vs 15.428 ± 1.718 , $p = 0.0052$). *Supplementary Movie 1* further confirms the significant difference between the control and TENG-driven EA group at 4 wpi. Furthermore, there is no significant difference between the positive control and TENG-driven EA system.

TENG-driven EA treatment stimulated locomotion recovery

Catwalk™ is an automated gait analysis system, which provides an unbiased quantitative assessment of locomotor function and detects detailed differences in SCI rats [51,52]. The overview of each group's gait at 4 weeks after injury is shown in Fig. 4a. And the overviews of each group's gait at different timepoints are shown in Fig. S4–Fig. S7, and *Supplementary Movie 2–5*. As one of the most frequently used parameters in the catwalk system [53], stride length describes the distance between two consecutive paw placements of the same paw (Fig. 4b). However, there is no significant difference among the four groups (data not shown).

We next investigated the step pattern and quantitative analysis revealed that the TENG-driven EA system led to a significant increase in the regularity index (TENG-driven EA group versus control group: 3 wpi, $p = 0.0232$; 4 wpi, $p = 0.0045$) (Fig. 5a and b). In addition, the TENG-driven EA group has an increase in the rate of diagonal support, which was considered as the natural gait pattern [54]. Nevertheless, whichever EA treatment groups has a higher diagonal support rate compared to the control group at 4 wpi (Fig. 5c). Cadence reflects the frequency of steps during a trial. The TENG-driven EA treatment significantly increased the frequency of steps at both 2 wpi and 4 wpi, respectively (Fig. 5d). Moreover, the average speed in the TENG-driven EA group also increased obviously at 4 wpi compared with the control group. ($p = 0.0416$). And the average speed in the TENG-driven EA group was equivalent to the positive control group ($p = 0.7599$). (Fig. 5e).

TENG-driven EA treatment inhibited neuron death and astrocyte reactivity.

Trauma to the spinal cord results in extensive apoptotic cells including neurons and glial cells [55]. We first examined the effect of TENG-driven EA treatment on the survival of neuron in the ventral horn. After SCI, a massive loss of neurons was observed in the control group compared with the sham group. However, TENG-driven EA group alleviated neurons loss in caudal to the lesion site when compared with the control group after injury ($p = 0.0060$; 0.0003 ; < 0.0001 ; respectively). Furthermore, there was no significant difference between the positive control and TENG-driven EA group in 400, 800, and 1200 μm caudle to the lesion site ($p = 0.6320$; 0.9839 ; > 0.9999 ; respectively) (Fig. 6a and b).

Astrocytes pose a double-edged sword in SCI. In the acute period, they help to contain the inflammation and thus prevent the expansion of inflammation [56]. While exposure to the microenvironment post-injury, astrocytes become reactive marked by varying upregulation of the intermediate filament decorating

proteins glial fibrillary acidic protein (GFAP) [57]. The increase in GFAP helps scar-forming astrocytes to form a rigid, densely bundled structure around the lesion and finally form the glial scar [58]. The glial scar is the physical and chemical barrier to axon regeneration [59]. In addition, astrocytes produce inhibitory ECMs as a response to a variety of different cells and molecular triggers [60,61]. Therefore, astrocyte overactivation is detrimental to spinal cord repair. TENG-driven EA treatment significantly decreased the mean fluorescence intensity of GFAP in astrocytes compared to the control group (Fig. 6c). And significant differences were found at 800 and 1200 μm caudle to the lesion site. ($p = 0.0105$; < 0.0001 ; respectively) (Fig. 6d). Collectively, these dates indicated that EA inhibits neuron death and astrocyte overactivation after SCI.

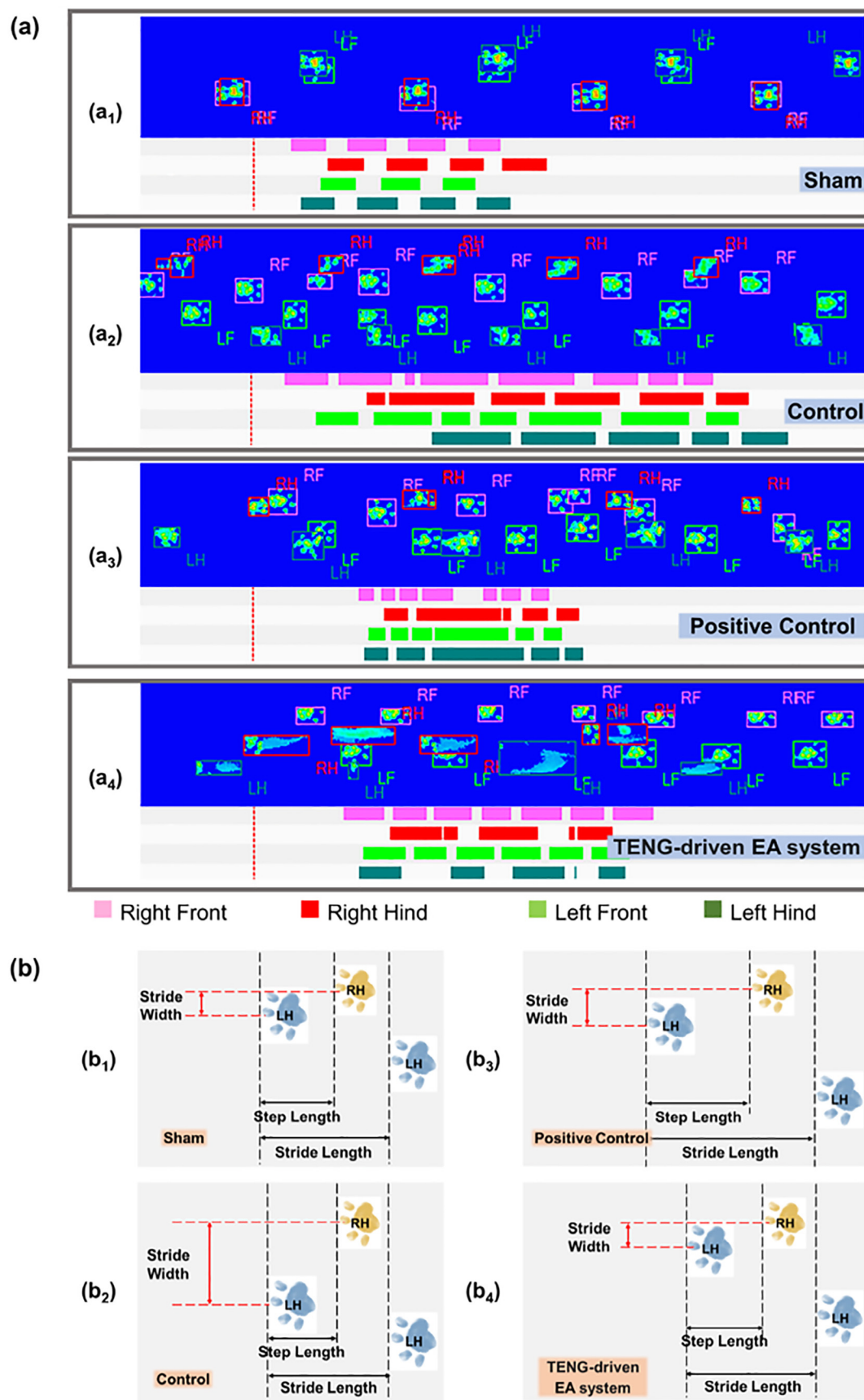
Conclusion

In summary, we propose a traditional Chinese medicine acupuncture treatment with the assistance of TENG technology, which can promote the recovery of the nervous system and motor function after SCI in rats. This treatment utilizes a soft-contact FR-TENG to generate an effective current stimulation that acts on two effective acupoints (Dazhui, GV14; Mingmen, GV4) by inserting electric needles. Compared to a continuous unidirectional current of commercial EA instruments, the TENG-driven EA system exhibits a continuous bidirectional current. More importantly, the needle handles of the TENG-driven EA system also show significant shaking at 200–250 rpm, indicating that the FR-TENG can be used as a kind of current generator to provide a continuous controlled current with a specific amplitude for acupuncture. The TENG-driven EA treatment enhances neuron survival in the ventral horn and inhibits astrocyte activation in the lesion site. Therefore, the TENG-driven EA treatment provides a significant neuroprotection against spinal cord contusion in rats. In addition, the behavior results show that locomotion functional recovery in the TENG-driven EA group. Different waveforms (such as the discontinuous wave and dilatational wave) remain to be explored for a more targeted treatment of patients. The comprehensive results of this work indicate that the TENG-driven EA treatment is expected to play an important role in the application of Chinese medicine acupuncture.

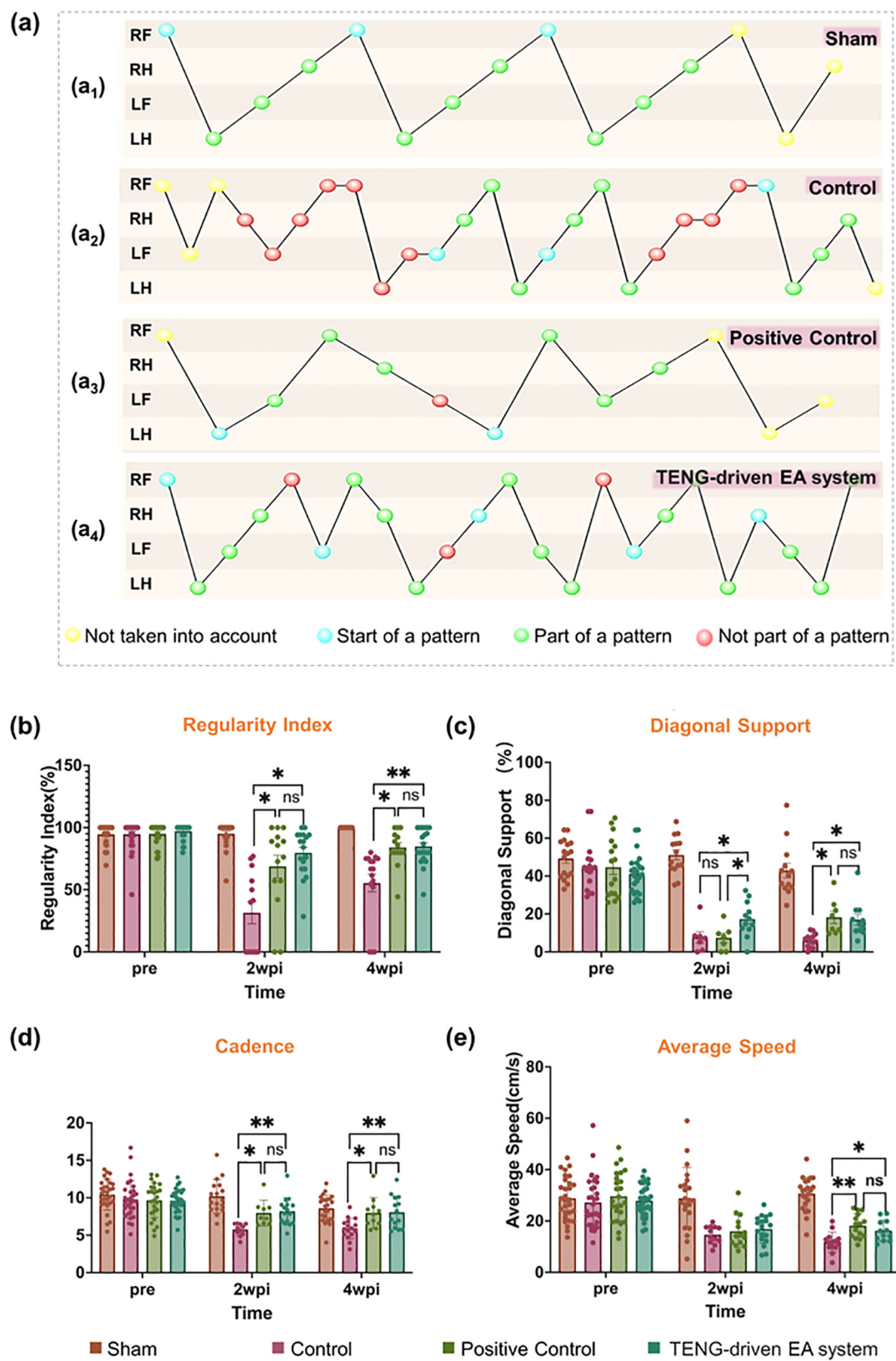
Experimental section

Fabrication of the soft-contact FR-TENG

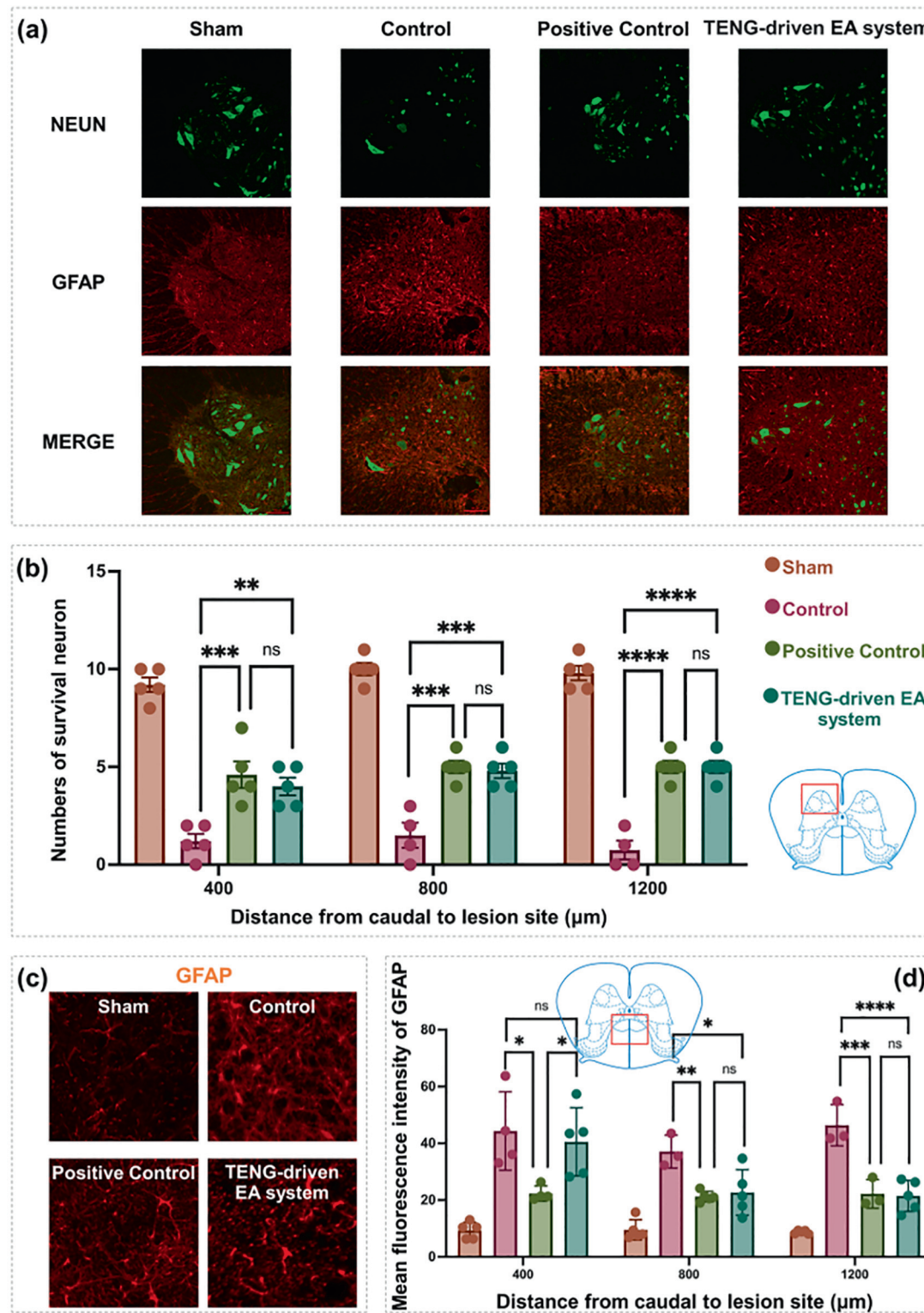
The soft-contact FR-TENG consisted of two parts: a rotator and a stator. For the rotator, an acrylic disk of 200 mm in diameter was cut by a laser cutter (PLS6.75, Universal Laser System) and was finely hollowed out at an interval of 30°, while a concentric circle (diameter: 30 mm) was cut at the center of the acrylic disk. Twelve FEP films with a thickness of 50 μm were successively fixed to the cutting pores of the acrylic substrate as the triboelectric dielectric layer. To ensure the elasticity of the soft FEP film for more full contact with the stator, a Kapton film of the same size with adhesive (thickness: 120 μm) has adhered to the back of the FEP film. The stator was made of a printed circuit board (PCB) with interdigital copper electrodes and a corresponding acrylic sheet as the supporting substrate. The diameter of both the PCB with copper electrodes and the acrylic substrate is 200 mm.

**FIGURE 4**

Footprint of the sham, control, positive control, and TENG-driven EA group. (a) Representative images of all groups' gait overview. (b) The stride length, stride width, step length of each group.

**FIGURE 5**

TENG-driven EA treatment improved motor function recovery. (a) Representative step pattern images of sham, control, positive control, and TENG-driven EA system group. (b) Regularity index (%) is an index for the degree of interlimb coordination during gait. (c) Diagonal support is the percentage of using 2 diagonal paws simultaneously for support. (d) Cadence reflects the frequency of steps. (e) Average speed represents the average distance that the animals walk per second. * $p < 0.05$, ** $p < 0.01$, as determined by one-way ANOVA analysis.

**FIGURE 6**

TENG-driven EA treatment inhibited neuron death and Astrocyte activation. (a) Representative fluorescence images of transverse spinal cord sections showing GFAP (red) and NEUN (green). Bar = 100 μ m. (b) Quantification of the number of survival neuron. $*p < 0.05$, $**p < 0.01$, as determined by one-way ANOVA analysis. (c) Representative fluorescence images of transverse spinal cord sections showing GFAP (red). Bar = 20 μ m. (d) Quantification of GFAP mean fluorescence intensity. Data are shown as the means \pm SD. $*p < 0.05$, $**p < 0.01$, as determined by one-way ANOVA analysis.

Electrical measurement and characterization of the FR-TENG and the commercial EA apparatus

A commercial brushless motor (BLM230HP-AS) was utilized to drive the rotary process of the FR-TENG. A transformer (Beijing Yaohua Dechang Electronics Co., Ltd, PE 2006 220-12-0.35 VA) was used in the circuit to increase the stimulated current. The V_{oc} , I_{sc} , Q_{tr} , and the current waveform were measured by a programmable electrometer (Keithley 6514). A commercial EA instrument (Shantou Medical Equipment Factory Co., Ltd, 6805-A) was applied to serve as an experimental positive control group.

Animals and groups

Adult female Sprague-Dawley rats ($n = 40$), weighing 200 ± 10 g, were used in this study. They were housed in animal housing on a 12:12 h light-dark cycle with water and food provided ad libitum. All procedures were approved by the Animal Experiment Ethics Committee of Chongqing Medical University. The animals were randomly divided into four groups (1) sham group, (2) control group (without treatment), (3) positive control group, and (4) TENG-driven EA group.

Spinal cord injury

The rats of control group, positive control group and TENG-driven EA system group were anesthetized with 1% pentobarbital sodium (5 ml/kg). The spinal cord was exposed by a laminectomy at the T9-T11 level without disrupting the dura. To stabilize the spine, the spinous processes of T8 and T12 were clamped. The exposed dorsal surface of the spinal cord was subjected to contusion injury ($10\text{ g} \times 2.5\text{ cm}$) using Allen's impactor. For the sham-operated rats, the rats underwent a T9-T11 laminectomy without contusion injury.

Electroacupuncture treatment

Rats received EA treatment at Dazhui (GV14, located on the posterior midline below the spinous process of the seventh cervical vertebra) and Mingmen (GV4, located on the posterior midline below the spinous process of the second lumbar vertebra) 12 ~ 24 h after SCI. The rats were bound in prone position and EA was applied to the positive control group and the TENG-driven EA group with 6805-A electric acupuncture or TENG-driven EA system five times a week for 2 weeks. Each EA treatment lasted 30 minutes. Disposable sterile acupuncture needles (DONG BANG Acupuncture Needle 0.3 mm × 30 mm) were used in this study.

Behavioral test

The open-field Basso-Beattie-Bresnahan (BBB) scoring system was used to evaluate the recovery of hindlimb locomotor function. Examination of functional deficits was conducted at 1, 3, 7, 14, 21 and 28 days after spinal cord injury. In brief, rats were placed on a flat surface and observed for 3 min by two trained investigators. The investigators were blind to the experimental conditions and simultaneously evaluated animal behavior. A score of 0 represents no observed hindlimb movements, and a score of 21 represents normal gait.

In addition, the Catwalk test was used to get a quantitative gait analysis. An enclosed glass walkway was illuminated with

fluorescent light coming from the side. The light reflected by the rat's paws as they contacted the walkway was captured by a highspeed video camera and then transformed into a digital image. All animals underwent a Catwalk XT automated quantitative gait analysis every day for 3 days and the baseline was taken 1 day before SCI. The Catwalk test was conducted every-two weeks after SCI until sacrificed. Footprints were automatically or manually labeled as left fore (LF) right fore (RF), left hind (LH), and right hind (RH) paws. After identification of all individual footprints, data including Average Speed, Cadence, Diagonal Support, and Regularity Index were all automatedly analyzed and exported.

Immunofluorescence staining

Tissue preparation

All rats were sacrificed 4 weeks after SCI. They were perfused firstly with 0.01 M phosphate-buffered saline (PBS) followed by 4% paraformaldehyde (PFA). The spinal cord was dissected and post-fixed in 4% PFA for 24 h, dehydrated gradually with 0.1 M phosphate buffer containing increasing amounts of sucrose (18%; 24%; 30%) for 3–5 days, embedded in an optimal cutting temperature compound (Tissue-Tek Sakura) and finally frozen at -80°C . The spinal cord was sectioned transversely at a thickness of 16 μm .

Immunofluorescence staining

Tissue sections were taken from -80°C and thawed for 30 min at room temperature. After washing in PBS (0.01 M, pH = 7.4) for three times (8 min), sections were incubated in 0.03% Triton X-100 for 30 min, followed by three PBS washes (8 min). Then sections were incubated with donkey serum for 45 min. After that, appropriate primary antibodies were applied overnight at room temperature. On the following day, sections were washed in PBS three times (8 min) and subsequently incubated with secondary antibodies for 45 min at 37°C . Finally, sections were sealed in Antifade Polyvinylpyrrolidone Mounting Medium (Beyotime, China).

Primary antibodies

Rabbit anti-GFAP (1:2000, Thermo, USA); Guinea pig anti-NeuN (1:800, Millipore, USA).

Secondary antibodies; Donkey anti-rabbit 488 nm (1:400, Jackson Laboratories, USA); Donkey anti-rabbit 594 nm (1:400, Jackson Laboratories, USA); Donkey anti-guinea pig 488 nm (1:400, Jackson Laboratories, USA).

Statistical analysis

All data were presented as the mean \pm standard deviation (SD). Statistical tests used are the one-way ANOVA with Bonferroni's post-hoc analysis and two-way ANOVA followed post hoc Tukey's test. Statistical analyses were performed using the GraphPad Prism software (ver. 9.2). $p < 0.05$ was regarded as statistically significant.

Data and materials availability

The data that support the findings of this study are available from the corresponding author upon reasonable request.

CRediT authorship contribution statement

Xuelian Wei: Conceptualization, Methodology, Data curation, Investigation, Writing – original draft, Writing – review & editing. **Yunhang Wang:** Methodology, Visualization, Data curation, Investigation, Writing – original draft, Writing – review & editing. **Botao Tan:** Methodology, Data curation, Investigation, Writing – original draft, Writing – review & editing. **Enyang Zhang:** Data curation, Investigation. **Baocheng Wang:** Data curation, Investigation. **Hong Su:** Methodology, Investigation. **Lehua Yu:** Methodology, Investigation. **Ying Yin:** Supervision, Conceptualization, Writing – original draft, Writing – review & editing. **Zhong Lin Wang:** Supervision, Conceptualization, Writing – original draft, Writing – review & editing. **Zhiyi Wu:** Supervision, Conceptualization, Writing – original draft, Writing – review & editing.

Declaration of Competing Interest

The authors declare that they have no known competing financial interests or personal relationships that could have appeared to influence the work reported in this paper.

Acknowledgements

The authors sincerely appreciate the experimental platform support of the State Key Laboratory of Trauma, Burns and Combined Injury, Department of Research Institute of Surgery, Daping Hospital, Army Military Medical University. We thank Prof. Yuan Liu and Prof. Ce Yang for their advice on the current project. Botao Tan and Ying Yin were supported by the Kuanren Talents Program of the Second Affiliated Hospital of Chongqing Medical University. This work was supported in part by the National Natural Science Foundation of China (No. 81702221, No. 82002377); Natural Science Foundation of Chongqing (No. cstc2020jcyj-msxm0651, cstc2019jcyj-msxmX0195).

Appendix A. Supplementary data

Supplementary data to this article can be found online at <https://doi.org/10.1016/j.mattod.2022.09.010>.

References

- [1] Acupunct. Med. 15 (1997) 104–107.
- [2] M.J. Mallory et al., J. Integr. Med. 14 (2016) 311–314.
- [3] W. Yao et al., Math. Methods Appl. Sci. 43 (2020) 1555–1564.
- [4] U. Luis et al., Nature 589 (2021) 573.
- [5] I.-S. Lee et al., Acupunct. Med. 37 (2019) 375–377.
- [6] Y. Wang et al., Medicine 97 (2018) e11986.
- [7] H. Angus-Leppan et al., BMJ 368 (2020) m1096.
- [8] A.A. Gelfand et al., JAMA Intern. Med. 177 (2017) 516–517.
- [9] M. Xu et al., Stroke 49 (2018) e237–e238.
- [10] A. Meakins et al., Brit. J. Sport. Med. 51 (2017) 484.
- [11] S. Liu et al., Nature 598 (2021) 641–645.
- [12] P.-Y. Liu et al., J. Geriatr. Cardiol. 11 (2014) 303–310.
- [13] D. Amorim et al., Complement. Ther. Clin. 46 (2022) 101541.
- [14] F. Wang et al., Neurochem. Res. 33 (2008) 2023.
- [15] X. Yu et al., Inflamm. Bowel Dis. 28 (2022) e21.
- [16] J.D.Z. Chen et al., Neurogastroenterol. Motil. 30 (2018) e13393.
- [17] X. Chen et al., Adv. Funct. Mater. 30 (2020) 2004673.
- [18] G. Conta et al., Adv. Mater. 33 (2021) 2007502.
- [19] X. Xia et al., EcoMat 2 (2020) e12049.
- [20] Z.L. Wang, Mater. Today 20 (2017) 74–82.
- [21] F. Arab Hassani et al., ACS Nano 12 (2018) 3487–3501.
- [22] Y. Long et al., Adv. Sci. 8 (2021) 2004023.
- [23] S. Lee et al., Nano Energy 33 (2017) 1–11.
- [24] S. Lee et al., Nano Energy 60 (2019) 449–456.
- [25] H. Wang et al., Nano Energy 63 (2019) 103844.
- [26] C. Wang et al., Nanomaterials 12 (2022) 1366.
- [27] Z. Zhao et al., Nat. Commun. 11 (2020) 6186.
- [28] Z.L. Wang et al., Mater. Today 30 (2019) 34–51.
- [29] Z.L. Wang et al., Energy Environ. Sci. 8 (2015) 2250–2282.
- [30] S. Lee et al., Nano Energy 50 (2018) 148–158.
- [31] W. Hu et al., Nano Energy 57 (2019) 600–607.
- [32] G. Yao et al., ACS Nano 13 (2019) 12345–12356.
- [33] J. Wang et al., ACS Nano 13 (2019) 3589–3599.
- [34] R. Luo et al., Adv. Healthcare Mater. 10 (2021) 2100557.
- [35] Z. Liu et al., Adv. Mater. 33 (2021) 2007429.
- [36] R. Kumar et al., World Neurosurg. 113 (2018) e345–e363.
- [37] E. Gilbert et al., Cells 11 (2022) 846.
- [38] B. Yu et al., Science 370 (2020) 342–346.
- [39] H.J. Park et al., Exp. Neurol. 180 (2003) 93–98.
- [40] T. Wang et al., Medicine 99 (2020) e21077.
- [41] W. Cong et al., Ann. Palliat. Med. 10 (2021) 104–113.
- [42] A. Wong et al., Am. J. Phys. Med. Rehabil. 82 (2003) 21–27.
- [43] Y. Chen et al., Front. Immunol. 13 (2022) 788556.
- [44] Y. Xin et al., Acupunct. Med. (2022), <https://doi.org/10.1177/09645284221076515>.
- [45] X. Wang et al., Anat. Rec. 304 (2021) 2494–2505.
- [46] C. Tan et al., Anat. Rec. 304 (2021) 2506–2520.
- [47] W. Xiao et al., Neuropsychiatr. Dis. Treat. 15 (2019) 3429–3442.
- [48] K. Li et al., Neural Plast. 2020 (2020) 5474608.
- [49] M. Cheng et al., J. Mol. Neurosci. 70 (2020) 2031–2040.
- [50] B. Zhu et al., Nat. Commun. 5 (2014) 4523.
- [51] I.K. Timotius et al., eNeuro 8 (2021) 1–14.
- [52] M. Aceves et al., eNeuro 7 (2020) 1–9.
- [53] E. Kappos et al., Brain Eehav. 7 (2017) e00723.
- [54] L. Mészáros et al., Acta Neuropathol. Commun. 9 (2021) 68.
- [55] C. Ahuja et al., Nat. Rev. Dis. Primers 3 (2017) 17018.
- [56] A. Tran et al., Physiol. Rev. 98 (2018) 881–917.
- [57] K.X. Xu et al., Glia 25 (1999) 390–403.
- [58] B. Xu et al., Neurobiol. Dis. 73 (2015) 36–48.
- [59] C. Chen et al., Exp. Neurol. 278 (2016) 27–41.
- [60] M. Hara et al., Nat. Med. 23 (2017) 818–828.
- [61] C. Schachtrup et al., J. Neurosci. April. 30 (2010) 5843–5854.